Investigation of mechanical properties of AlSi3Cr alloy

Marialaura Tocci, Annalisa Pola, Lorenzo Montesano, G. Marina La Vecchia
Department of Mechanical and Industrial Engineering, University of Brescia, Via Branze 38, 25123, Brescia, Italy
m.tocci@unibs.it, http://orcid.org/0000-0002-7515-0615
annalisa.pola@unibs.it, http://orcid.org/0000-0002-0722-6518
lorenzo.montasano@unibs.it, http://orcid.org/0000-0001-5465-6265
marina.lavecchia@unibs.it, http://orcid.org/0000-0001-5919-0396

Mattia Merlin, Gian Luca Garagnani
Department of Engineering (DE), University of Ferrara, Via Saragat 1, 44122, Ferrara, Italy
mattia.merlin@unife.it, http://orcid.org/0000-0003-4685-1073
gian.luca.garagnani@unife.it, http://orcid.org/0000-0002-5403-0868

ABSTRACT. In the present paper, microstructural and mechanical properties of an innovative AlSi3Mg alloy were studied. Particularly, the effect of the addition of Cr and Mn on tensile strength and impact toughness was evaluated. In fact, the presence of these elements leads to the formation of an intermetallic phase with a globular or polyhedral morphology. It was therefore investigated the role played by Cr-Mn containing particles in the failure mechanism and the influence of the heat treatment parameters. Moreover, tensile and impact tests were performed on A356 samples in T6 condition, whose results were compared with the performance of the innovative alloy.
Considering the static properties, the innovative alloy showed remarkable values of tensile strength, while ductility was improved only after heat treatment optimization. Poor impact toughness values were measured and the microstructural analysis confirmed the presence of coarse intermetallics, acting as crack initiation and propagation particles, on the fracture surfaces.

KEYWORDS. Al-Si-Mg alloys; Tensile test; Impact test; Fracture surface.

Citation: Tocci, M., Pola, A., Montesano, L., La Vecchia, G.M., Merlin, M., Garagnani, G.L., Investigation of mechanical properties of AlSi3Cr alloy, Frattura ed Integrità Strutturale, 42 (2017) 337-351.

Received: 11.08.2017
Accepted: 11.09.2017
Published: 01.10.2017

INTRODUCTION

In the last decades, the light weighting of cars and trucks has become a very widely discussed theme [1] in both academic and industrial world. The design of more efficient processes and the development of stronger and lighter materials enhance the reduction of weight of cars and trucks components, allowing the decrease of fuel consumption and toxic emissions in atmosphere. For such reasons, the use of aluminum alloys in transports is increasing in the last years. Among Al alloys, Al-Si-Mg alloys are the most used for automotive castings production [2,3] because of their excellent castability, good corrosion resistance, high elongation and significant strength.

In addition, the light weighting of automotive components can be achieved by enhancing the mechanical properties of Al alloys due to the presence of strengthening elements. For instance, Cr and Mn additions in Al-Si alloys lead to the formation of globular or polyhedral intermetallics [4-6], reducing the detrimental effect of the brittle needle-like β-Al_5FeSi intermetallics, thus increasing the mechanical properties of the material. In fact, in Al-Si alloys, Fe is a common impurity that forms brittle needle-like intermetallics, known as β-Al_5FeSi phase, which are harmful for mechanical properties, particularly for tensile and fatigue behavior [4,7,8].
In addition, heat treatment is also a key factor to consider in order to optimize the performance of any Al-Si-Mg alloy. At this regard, several authors examined the effect of heat treatment parameters, in particular solution and ageing (T6), and chemical composition on microstructure, mechanical properties and precipitation sequence for Al-Si-Mg alloys [9]. For instance, Wang et al. [10] studied the effect of Mg content on both solidification and precipitation behavior of AlSi7Mg casting alloy. The ageing behavior of Al-Si alloys with Mg and Cu addition was investigated also by Li et al. [11], who focused their attention on the precipitation sequence.
The presence of Cr and Mn in the alloy composition does not seem to interact significantly with Mg during ageing treatment. In fact, it was recently demonstrated that Cr-containing dispersoids already form in AlSi3Cr alloy during the solution treatment, without changes during ageing, and that they contribute to the dispersion hardening of the material [12].
Notwithstanding the abundant information in scientific literature about heat treatment of Al-Si-Mg alloys, for industrial production, it is mandatory to define the proper heat treatment for each alloy, in order to reach a good compromise between strength and ductility.
In the present paper, tensile properties and impact toughness of an innovative AlSi3Cr alloy were investigated before and after T6 heat treatment. The studied alloy is characterized by the presence of Cr and Mn in order to modify the morphology of intermetallic particles and improve material properties. This alloy was developed for the production of truck wheels by means of a non-conventional hybrid technique, which combines features of both low pressure die casting and forging processes [13]. Nevertheless, the presence of a significant amount of intermetallic phase can still represent a limit to the mechanical performance of the Cr-containing alloy and deeper investigations are needed to evaluate its effect.
The influence of time and temperature of the ageing treatment were analyzed, paying particular attention to the role of intermetallics. Furthermore, in order to better evaluate the suitability of the alloy for this application, the obtained results were compared to the properties of the commercial A356-T6 casting alloy, currently used for the production of wheels.

MATERIALS AND METHODS

The content of main alloying elements in the studied alloy is shown in Tab. 1. The values are given in wt. % and were measured by optical emission spectrometer. As mentioned in the introduction, the chemical composition is between those of the conventional alloys for LPDC and forging. In fact, the alloy under investigation is an Al-Si-Mg alloy developed for the production of truck wheels by a non-conventional hybrid technique [13], combining features of both low pressure die casting (LPDC) and forging processes. Furthermore, Cr and Mn are present as main alloying elements. Ti was used as refining element, while no modifiers were added to the melt. A proper degassing was performed before casting.

	Si	Mg	Cr	Mn	Fe	Ti	Al
AlSi3Cr	3.158	0.558	0.276	0.120	0.123	0.115	Balance

Table 1: Main alloying elements (wt. %) for the studied alloy.

Samples to be tested in as cast conditions were directly machined to the proper shape for tensile and Charpy impact tests, while the other samples were first machined as cylinders, heat treated and then machined to the final shape according to the standards. All the samples were taken from the rim of the wheel in order to guarantee a reliable comparison of mechanical properties.
Solution and aging treatments were performed in air in laboratory furnaces. Solution temperatures were chosen according to solidus temperature measured by differential scanning calorimetry (DSC) [13], while aging temperatures were selected as suggested by good practice for this group of aluminum alloys [14]. Samples were solution treated for 3 h at 545 °C,

then water quenched at 65 °C [14] and subsequently aged at 165 °C and 190 °C for 1, 2, 4, 6 and 8 h. Between quenching and ageing treatments, the samples were kept at -20 °C in order to avoid natural ageing. During the heat treatment, the temperature was additionally monitored by a thermocouple placed inside an aluminum sample in the furnace chamber.
Microstructural characterization was carried out by both a Leica DMI 5000 M optical microscope (OM) and a LEO EVO 40 scanning electron microscope (SEM), equipped with an energy X-ray dispersive spectroscopy microprobe (EDS). In addition, the sludge factor referred to the Cr-Mn-rich intermetallic phase was calculated, while its average area fraction and morphology (roundness, average particle area, equivalent diameter, and maximum size) were investigated by image analysis techniques. In particular, roundness was evaluated as follows:

$$Roundness = \frac{P^2}{4\pi A} \tag{1}$$

where P is the perimeter and A is the area of each intermetallic compound. According to the formula, a value of roundness equal to 1 corresponds to a circle and it represents the minimum value: the more elongated the shape, the higher the roundness value.
Vickers microhardness tests were performed on as cast, quenched and aged samples using a Shimadzu indenter with an applied load of 200 g and a loading time of 15 s. In order to guarantee a reliable statistic, at least 20 measurements were carried out on each sample.
Tensile tests were performed at room temperature on as cast, quenched and aged samples using an Instron 3369 testing machine with a load cell of 50 kN. The crosshead speed was 1 mm/min in the elastic field and 2 mm/min in the plastic field. Accurate elongation values were obtained using a knife-edge extensometer fixed to the gauge length of the specimens. After tensile tests, in order to define the optimum heat treatment condition, the quality index (QI) was calculated starting from the values of ultimate tensile strength (UTS) and elongation (El%), using the following formula [15]:

$$QI = UTS + 150\log\left(El\%\right) \tag{2}$$

Charpy impact tests were performed at room temperature on U-notched samples with standard dimensions of 10 mm x 10 mm x 55 mm. In order to consider the effect of the heat treatment on the impact strength performance of the alloy, samples were tested in as cast, quenched and aged conditions. A CEAST instrumented pendulum with an available energy of 50 J was used and data were acquired by means of a DAS 64k analyzer. In this work, only the total energies absorbed by the specimens in the different thermal conditions are correlated with the microstructural features.
Tensile and impact strength tests were also performed on samples machined from a commercial A356 LPDC wheels in the T6 condition in order to compare the results with those of the innovative AlSi3Mg alloy.
The fracture cross-sections and surfaces of tensile and impact specimens were observed and analyzed by optical microscopy (OM) and scanning electron microscopy (SEM), respectively.

RESULTS AND DISCUSSION

Microstructural analysis and morphological analysis of intermetallics

The microstructure of the AlSi3Cr alloy in the as cast condition is reported in Fig. 1 at two different magnifications. It consists of a primary dendritic phase with a small amount of a eutectic mixture. Moreover, intermetallic particles with a globular or polyhedral morphology can be frequently detected (see arrows in Fig. 1b).
The chemical composition of this phase was evaluated by SEM-EDS analysis (Fig. 2 and Tab. 2). These particles are usually referred as the α-Al(Fe,Mn,Cr)Si intermetallic phase, which forms when Cr and/or Mn are added to the alloy composition [6,16].
After heat treatment, the typical spheroidisation and coarsening of the Si eutectic particles take place (Fig. 3b). In addition, as explained in a previous work by the authors [12], during solution treatment Cr-containing dispersoids also form in the aluminum matrix. It was demonstrated that they are responsible of an increase in material hardness and influence both tensile properties and toughness [7,8,17]. Intermetallic particles are not significantly affected by the heat treatment [18].

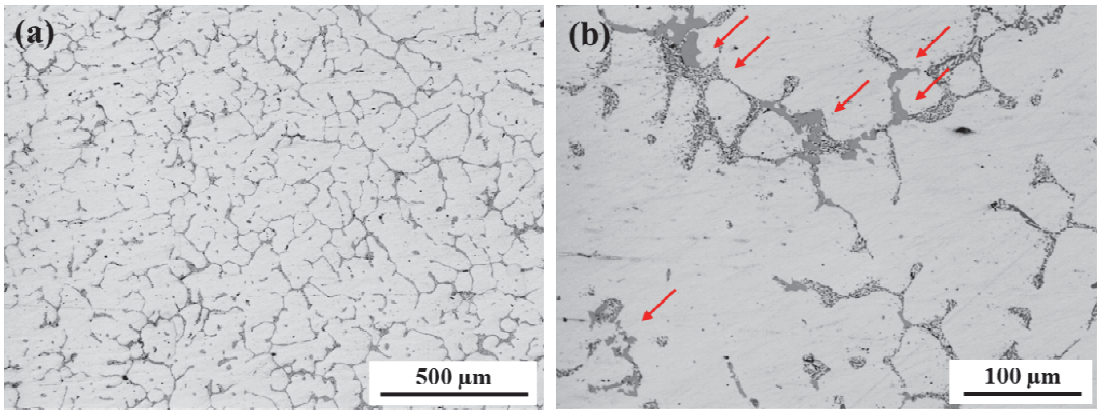

Figure 1: Typical microstructure of the innovative alloy in the as cast condition at two different magnifications.

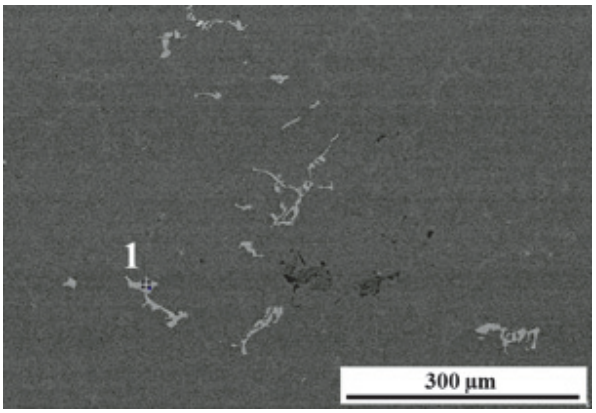

Figure 2: SEM micrograph of the AlSi3Cr alloy in the as cast condition.

	Al	Si	Cr	Mn	Fe
α-Al(Fe,Mn,Cr)Si phase	64.71	11.55	10.12	3.60	10.03

Table 2: Semi quantitative EDS analysis of the intermetallic compound shown in Fig. 2.

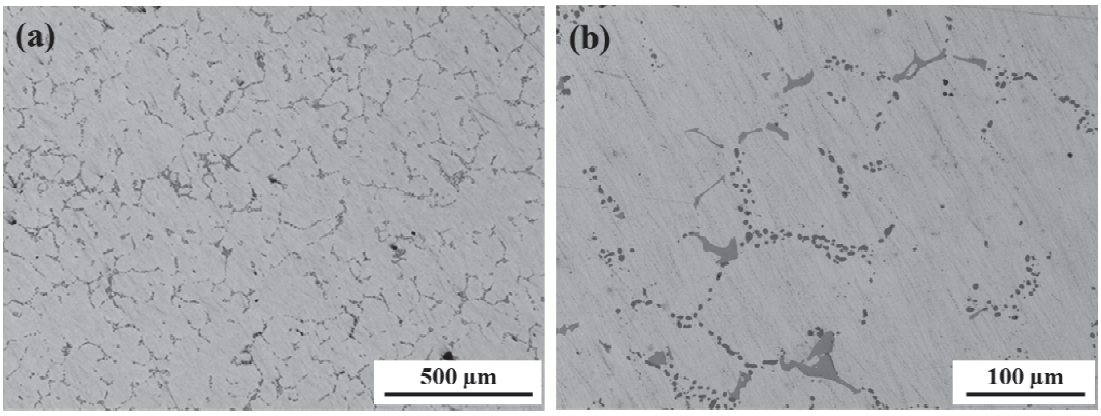

Figure 3: Typical microstructure of the AlSi3Cr alloy in aged condition (1 h at 165°C) at two different magnifications.

High-density intermetallic phases can precipitate as sludge and settle at the bottom of the furnace [19,20]. Hence, a sludge factor was defined in order to predict the formation of sludge according to the content of Fe, Mn and Cr for Al-Si-Cu

alloys and to estimate if the sedimentation of this phase is likely to happen in the molten metal [19,20]. Considering the chemical composition, a sludge factor of 1.19 was calculated for the AlSi3Cr alloy, according to Jorstad [19,20] and Gobrecht [20], and it resulted lower than the critical level causing sludge sedimentation [5].
In addition, according to [21], the sludge factor can be correlated to the area fraction of the intermetallic particles and not to their morphology, so the former parameter was calculated by means of image analysis technique. It was measured an average area fraction of α-Al(Fe,Mn,Cr)Si intermetallic phase of about 0.6 % and a particle density of 56 particles/mm^2. Additionally, the image analysis results pointed out that this phase is characterized by an average roundness of 2.75. A more accurate evaluation of the results showed that 70 % of the particles analyzed are characterized by a roundness value lower that 3, while about 30% of the intermetallics can reach a roundness above 3 up to 6. Particularly, very elongated intermetallics, with roundness between 5 and 6 represented only 2 % of the total investigated particles. These particles can play an important role during tensile tests since it is known that their sharp edges can behave as stress concentration points and therefore can lead to fracture [6]. All the discussed results are summarized in Tab. 3.

Morphological parameters for intermetallic particles		
Total area of intermetallics	0.05	mm^2
Area Fraction	0.6	%
Particles density	56	n° particles/mm^2
Average Roundness	2.75	-
Average particle area	106	µm^2
Equivalent diameter	11	µm
Maximum size	80	µm

Table 3: Image analysis results referred to the α-Al(Fe,Mn,Cr)Si intermetallic particles in AlSi3Cr alloy.

Hardness and tensile properties

The average values of Vickers microhardness and of tensile properties of the AlSi3Cr alloy in as cast condition are summarized in Tab. 4. The standard deviation of the measured properties is also reported.

	HV0.2	UTS (MPa)	YS (MPa)	El (%)
Average	73	202	106	5.3
Standard deviation	2	2	2	0.5

Table 4: Average mechanical properties of the AlSi3Cr alloy in the as cast condition.

The influence of the aging time on the Vickers microhardness of the studied alloy for the two considered aging temperatures, 165 °C and 190 °C, is shown in Fig. 4. As expected, it appears that the peak condition is reached earlier when ageing is performed at 190 °C rather than at 165 °C [9]. In fact, in the former case peak hardness is reached after 4 h and in the latter case after 6 h of treatment. Accordingly, over ageing occurs earlier when the heat treatment is performed at higher temperature, while the peak hardness is about 130 HV0.2 for both the ageing temperatures.
In order to investigate the evolution of the mechanical properties of the innovative alloy according to the aging time, tensile tests were performed on specimens in the same heat-treated conditions. It was found that the AlSi3Cr alloy shows a remarkable increase in strength after the ageing treatment, reaching values of UTS between 320 and 360 MPa and values of YS between 275 and 330 MPa (Fig. 5a-b). On the other hand, as expected as drawback of any increase in material strength, an inverse correlation between ductility and mechanical properties was found. In most heat-treated conditions, the AlSi3Cr alloy shows poor elongation values. However, as shown in Fig 5c, it is possible to reach elongation values between 4 % and 6 % with ageing treatments between 1 h and 4 h at 165 °C.

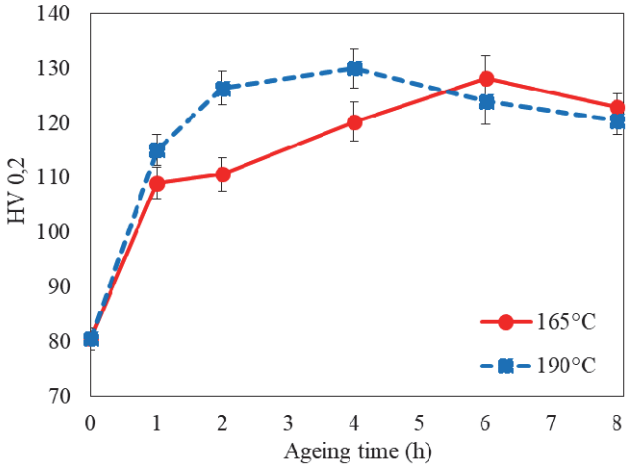

Figure 4: Ageing curves of AlSi3Cr alloy for ageing at 165°C and 190°C [22]. The standard deviation is shown as error bars.

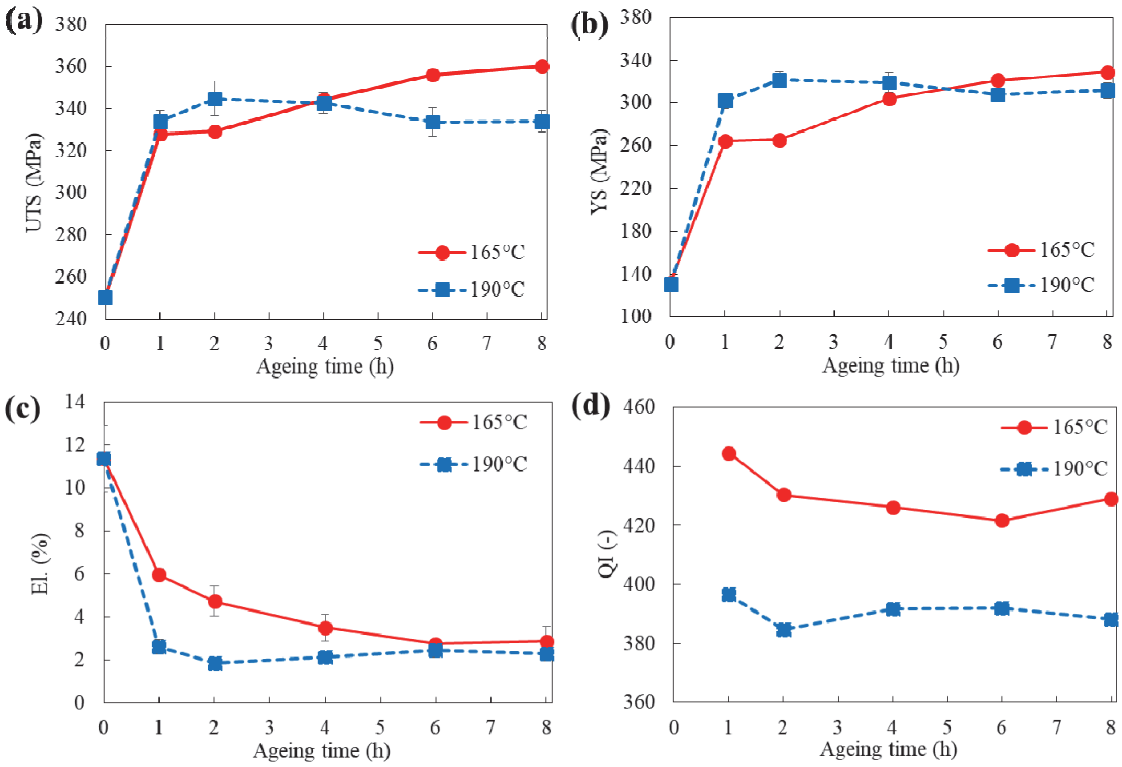

Figure 5: (a) UTS, (b) YS, (c) El and (d) QI of the AlSi3Cr alloy in the selected heat-treated conditions.

Microstructural analysis of tensile specimens

The loss in elongation at fracture can be explained considering that material ductility is affected by different parameters such as the presence of brittle Si eutectic particles, α- Al(Fe,Mn,Cr)Si intermetallics, Cr-containing dispersoids and Mg_2Si precipitates after heat treatment. Particularly, in as cast condition brittle Si particles and Fe-containing intermetallics are known to be responsible for crack propagation during the evolution of the fracture processes [7]. During heat treatment, as above mentioned, spheroidisation of Si particles and formation of Mg_2Si precipitates take place. The former is reported to be positive for tensile properties [23], while the latter is responsible of a loss in ductility of the α-Al matrix [9].

A mainly ductile fracture mechanism of the matrix is observed from SEM analysis of the fracture surfaces after tensile tests in all the selected heat-treated conditions (Fig. 6). A transcrystalline fracture, typical for Al-Si alloys [24] with visible traces of micro-deformation (dimples), can be observed.

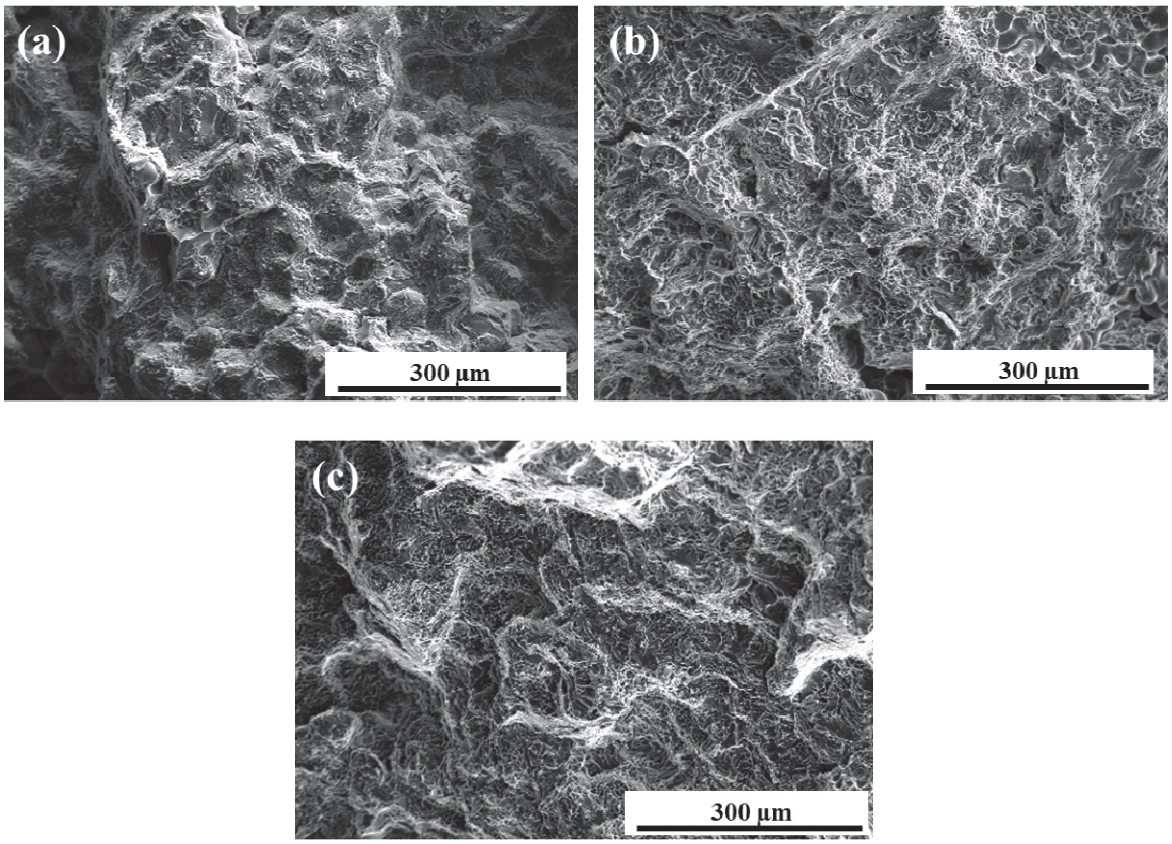

Figure 6: Fracture surface of AlSi3Cr tensile samples in (a) as cast, (b) as quenched and (c) aged condition (165°C).

As shown in Fig. 7a-b, intermetallic particles containing Fe, Mn and Cr were sometimes detected on the fracture surfaces; the EDS results of the identified particles are reported in Tab. 5. They appear to be small and not cracked and this supports the hypothesis that they play a marginal role in the fracture initiation. As reported by some authors [8,25,26], during tensile tests α-Al(Mn,Cr,Fe)Si intermetallics are not cut by dislocations, which instead create a circle around the particles and moves around them during tensile tests, bypassing the obstacle. It is believed that the same mechanism is taking place for the studied alloy, in particular when globular intermetallic particles are present.

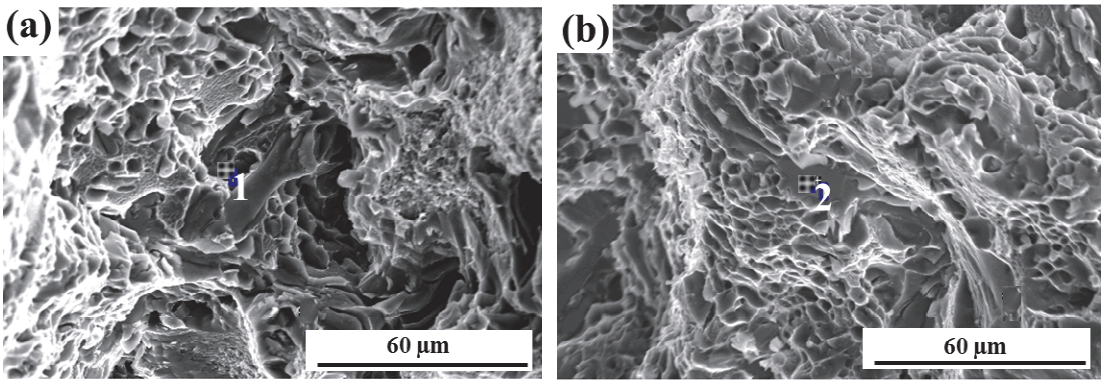

Figure 7: Intermetallic particles on the fracture surface of AlSi3Cr tensile samples in (a) as cast and (b) aged condition (165 °C).

	Mg	Al	Si	Cr	Mn	Fe
1	--	54.96	9.20	12.16	6.05	17.64
2	--	40.55	--	14.84	10.21	34.40

Table 5: EDS analysis (wt. %) of the intermetallic particles shown in Fig. 7.

Therefore, the main failure mechanism involves the fracture of eutectic Si particles rather than of intermetallics particles, as also visible from the two micrographs of the fracture profile of a specimen aged for 1 h at 165 °C (Fig. 8a-b); the fracture mainly follows the eutectic path. Nevertheless, also some cracked intermetallic particles could be present along the fracture surface (Fig. 8b), but they do not appear to strongly contribute to the fracture initiation and propagation.

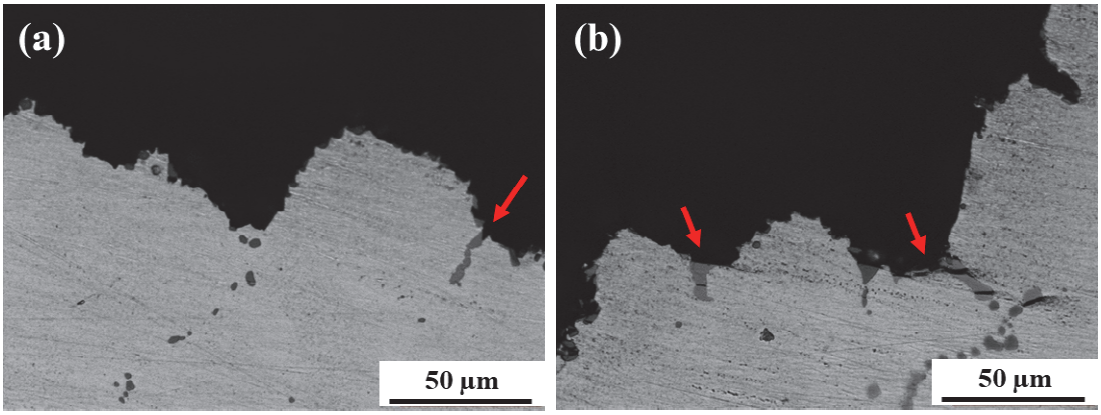

Figure 8: Cross section of fractured tensile specimen in aged condition (1h at 165°C).

This supports what is already reported by different authors about the positive contribution to tensile properties of the modification of intermetallic morphology due to Cr and Mn addition to Al-Si-Mg alloys [7,8,17]. Intermetallic particles seem to be not so critical for the tensile strength of heat-treated AlSi3Cr alloy, while most of the ductility loss is probably correlated to precipitation of hardening Mg_2Si particles. Unfortunately, it is not possible to identify
Cr-containing dispersoids on the fracture surface due to its non-regular morphology, even though their presence in the Al matrix was demonstrated in a previous study [22].

Impact strength results

During impact tests, the maximum load (Fm) was measured and the total impact energy (Wt) was calculated as the integral of load-displacement curve from the start to the end of the test, which is considered when the load comes to 2 % of its peak. The two complementary contributions to the total energy, i.e. the energy at the maximum load (Wm) and the propagation energy (Wp), were also calculated.
As an example, in Fig. 9 are reported the load-displacement curves of two selected specimens, one tested just after solution treatment performed at 545 °C for 3 h and one after the same solution treatment and subsequent ageing carried out at 165 °C for 1 h. In Tab. 6 are collected the measured and calculated impact properties of the same specimens.
Considering the results reported in the table, a significant variation of the impact behavior of the material was observed performing the ageing treatment after solution. The aging treatment for 1 h at 165 °C increases the maximum load of about 30 %, but decreases the impact strength of about 58 %. Comparing the trend of the curves, the aged specimen shows higher maximum load, but lower displacement to fracture and displacement at the maximum load. The ratio between the propagation energy and the nucleation energy is lower after the ageing treatment, pointing out that the crack growth stability decreases.
The mean impact energies of samples in all the investigated conditions are summarized in Fig. 10. The mean value of total impact energy obtained on the U-notched samples in as-cast condition was equal to 2.43 ± 0.14 J and it is reported for comparison as dotted line in the same figure.

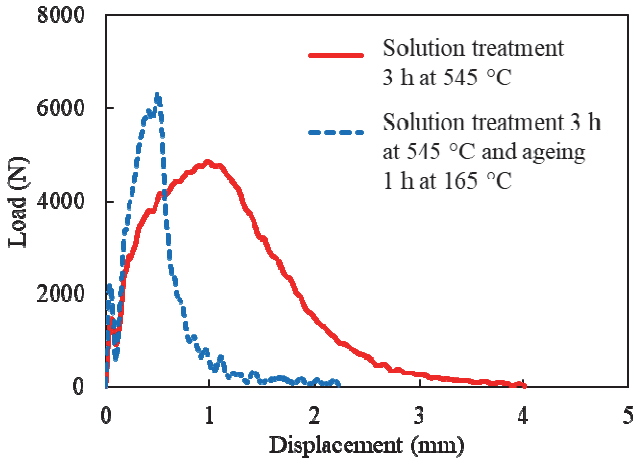

Figure 9: Instrumented impact strength curves of two selected specimens.

	Fm (N)	Wt (J)	Wm (J)	Wp (J)
As quenched condition (solution treated 3 h at 545 °C)	4844.05	7.63	3.46	4.17
Aged condition (solution treated 3 h at 545 °C and aged 1 h at 165 °C)	6327.93	3.19	1.88	1.31

Table 6: Measured and calculated impact properties from curves plotted in Fig. 9.

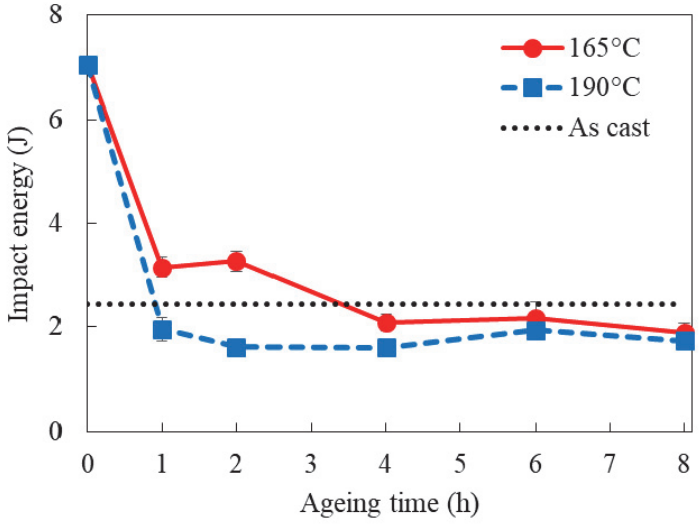

Figure 10: Total impact energy for AlSi3Cr samples in different conditions.

Solution treatment performed at 545 °C for 3 h increases impact energy values with respect to the as-cast condition (dotted
line in Fig. 10); this is mainly due to the spheroidisation of the eutectic Si particles and the dissolution of the coarse Mg_2Si particles during the solution treatment. It is well known, in fact, that solution treatment reduces the number of critical crack initiation points and therefore leads to the enhancement of the energy absorption during the impact [27]. Similarly, the partial decomposition of some Fe-containing intermetallics can positively contribute to increase the material toughness by diminishing sharp edges at the interface with the matrix. Nevertheless, after ageing treatment, a severe drop in impact strength takes place due to the precipitation of β'-Mg_2Si particles. These particles, with their brittle behavior, increase the

micro-stresses, reducing the α-Al strain: micro-cracks are more likely to originate [23,28,29,30]. The highest values of the absorbed impact energy were measured in the samples aged at 165 °C for short aging times, while after 6 and 8 h of ageing very similar values were recorded. In addition, almost constant values of the impact energy were found after ageing treatment at 190 °C, regardless of the aging time, probably due to the fast precipitation of the hardening Mg_2Si particles.

Microstructural analysis of impact strength specimens

Some significant SEM micrographs of the fracture surfaces of impact strength specimens are shown in Fig. 11. A typical micro-ductile morphology can be identified for the as cast and for the selected heat-treated conditions. Dimples formed around the Si eutectic particles due to the different ductility between the more deformable α-Al matrix and the less deformable Si particles.

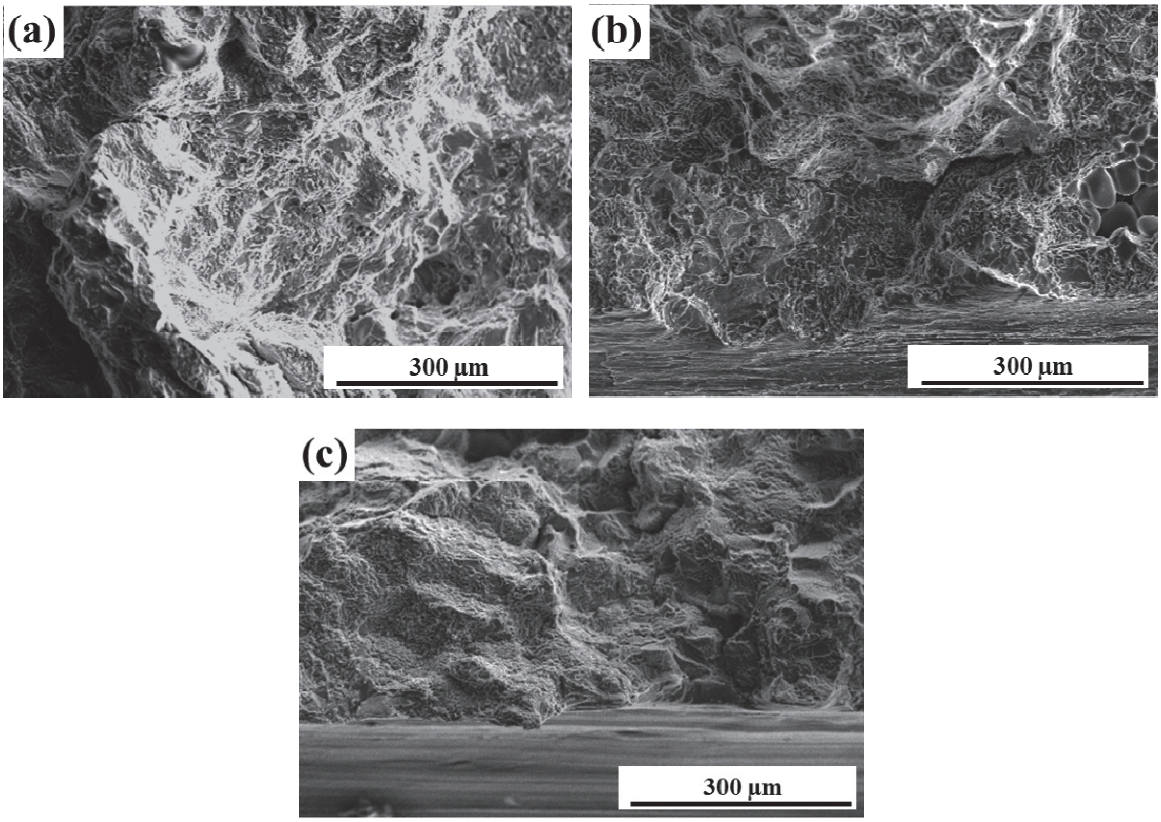

Figure 11: Fracture surfaces of AlSi3Cr impact strength specimens in (a) as cast, (b) as quenched and (c) aged condition (165 °C).

Several cracked and coarse intermetallics were observed on the fracture surfaces of the analyzed samples and some of them are pointed out in the micrographs of Fig. 12; the chemical composition of these particles, as evaluated by means of the EDS microprobe, is reported in Tab. 7. They surely play an important role in both crack initiation and propagation during the impact tests [27,30].

	Mg	Al	Si	Cr	Mn	Fe
1	0.67	91.89	4.18	1.34	0.48	1.44
2	--	61.20	13.47	9.91	4.15	11.26
3	--	66.19	8.58	10.48	4.05	10.71

Table 7: EDS analysis (wt. %) of the intermetallic particles pointed out in the micrographs of Fig. 11.

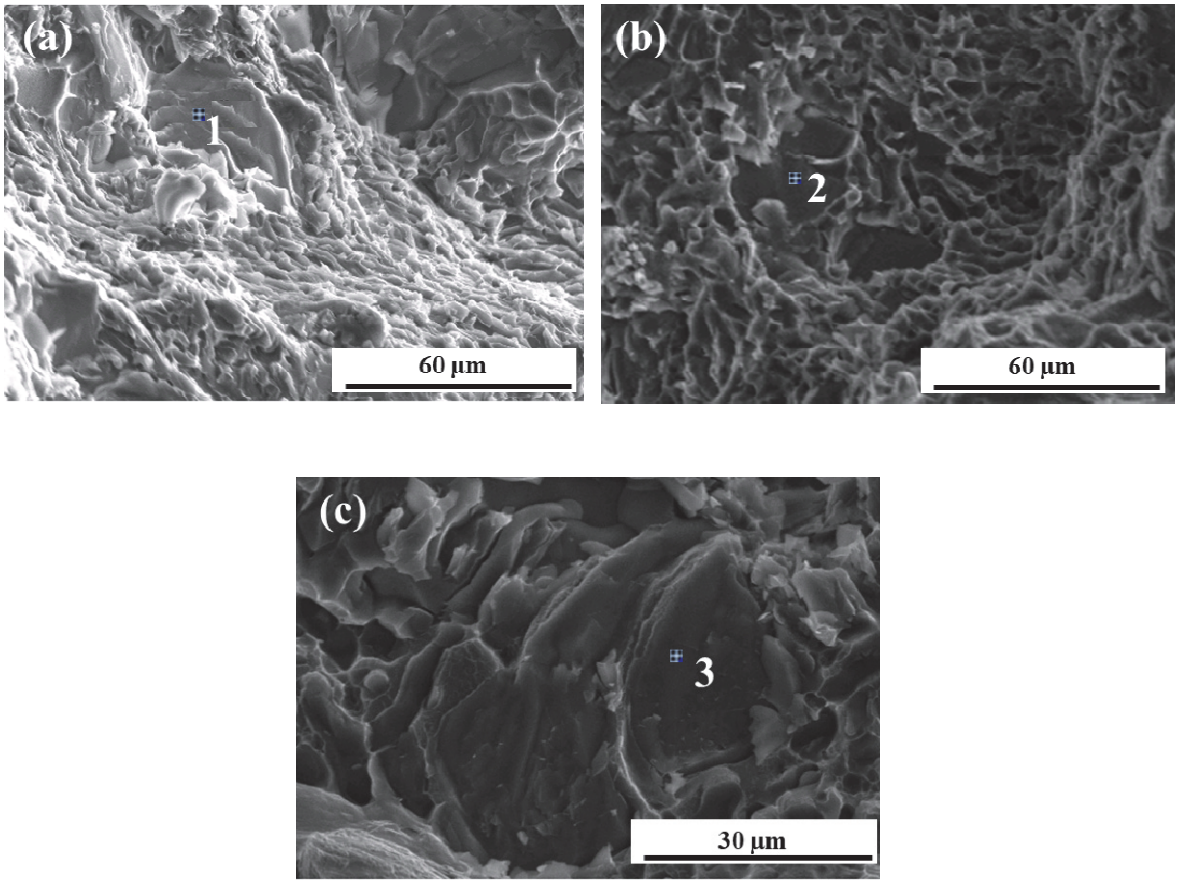

Figure 12: Cracked intermetallic particle on fracture surface of samples in (a) as cast, (b) as-quenched and (c) aged condition (165 °C).

Comparing the analyses performed on tensile and impact strength specimens, a significant increase in the number of intermetallics was observed on the fracture surfaces of the impact strength ones. The steep load variation during the impact tests probably induces the brittle behavior of the intermetallic particles. The intercrystalline fracture of eutectic Si crystals and of intermetallics is the cause of the fracture initiation. Then, after the principal crack is formed, the fracture seems to propagate following a quasi-claveage path along the intermetallics, as can be seen in Fig. 13.

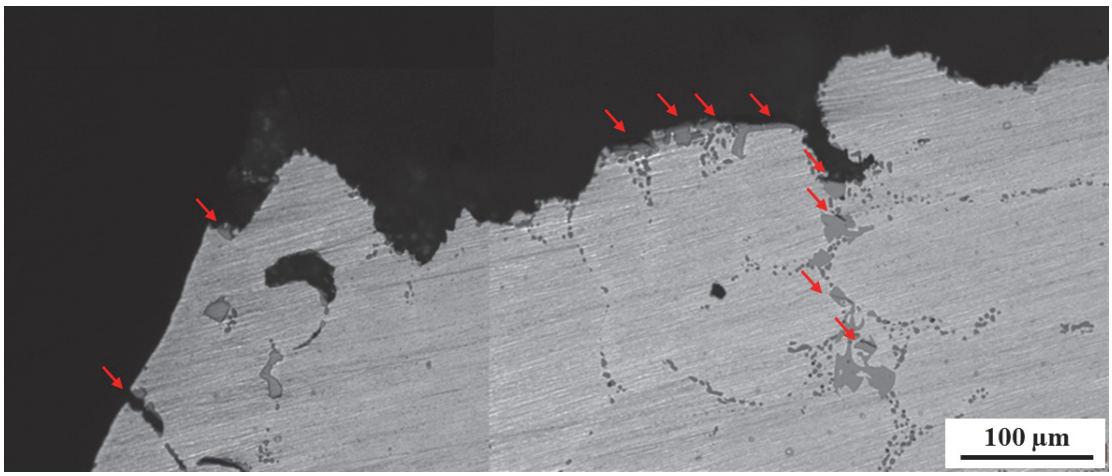

Figure 13: Fracture profile close to the notch of a fractured impact specimen in aged condition. The cracked intermetallic particles are indicated by red arrows.

Comparison with a conventional A356-T6 alloy

Tensile and impact strength tests were performed also on samples drawn from wheels produced by LPDC process with the traditional A356 alloy in the T6 condition (solution treatment at 540 °C for 4 h and ageing treatment at 155 °C for 2,5 h). In particular, the obtained results were compared with the performance of the innovative alloy in the best-considered heat-treated condition (ageing for 1 h at 165 °C). Data are collected in Fig. 14.

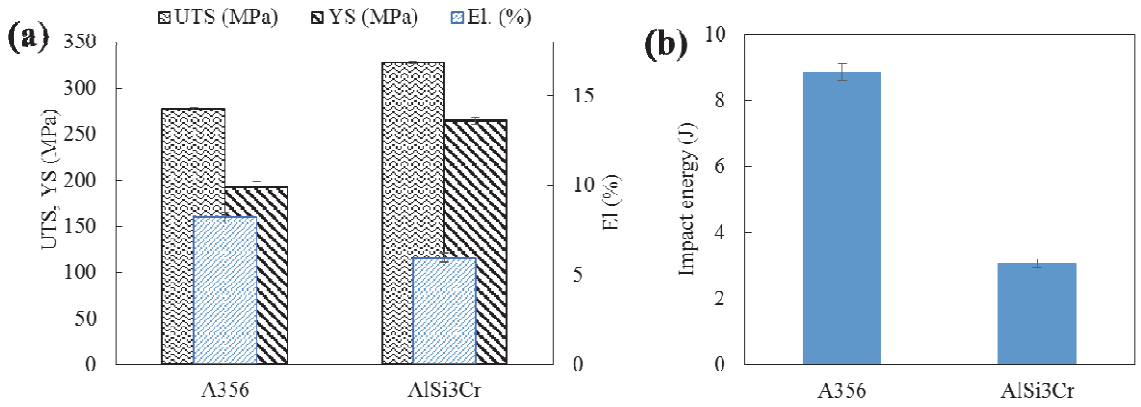

Figure 14: Average values of (a) tensile properties and (b) impact energy of A356-T6 alloy and AlSi3Cr (aging 1 h at 165 °C) alloy.

From the analysis of tensile properties, it can be observed that UTS and YS are significantly higher for the AlSi3Cr alloy than for the A356-T6 alloy (Fig. 14a). On the other hand, a slightly lower elongation is also recorded.

SEM micrographs of the fracture surface of a A356-T6 tensile specimen are shown in Fig. 15 at different magnifications. The morphology of the fracture surface is typically ductile (Fig. 15a) and some coarse Fe-containing platelet-like intermetallics can be observed on the fracture surface, as shown in Fig. 15b: the EDS analysis of the identified Fe-containing platelet is reported in Tab. 8. These intermetallics are characterized by sharp edges, surely inducing detrimental effects on the tensile properties [6].

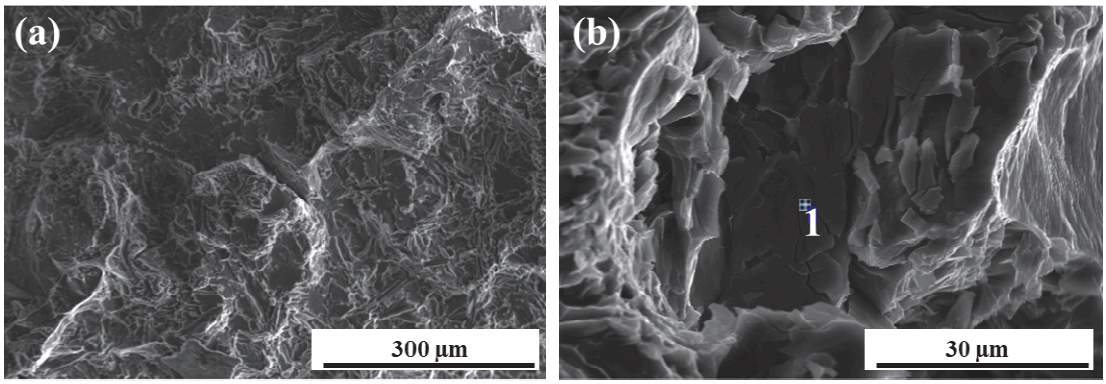

Figure 15: SEM micrographs of the facture surface of an A356-T6 tensile specimen.

	Mg	Al	Si	Fe
1	4.66	66.64	17.65	11.05

Table 8: EDS analysis (wt. %) of the intermetallic particle shown in Fig. 14.

Conversely, considering the comparison reported in the graph of Fig. 14b, the average impact energy absorbed by the A356-T6 alloy is significantly higher than the one of the innovative alloy in the best heat-treated condition. As previously shown in Fig. 12 and Fig. 13, the coarse secondary phases clearly identified on the fracture surfaces and on the fracture profiles play an important role in decreasing the impact strength of the heat-treated AlSi3Cr alloy.

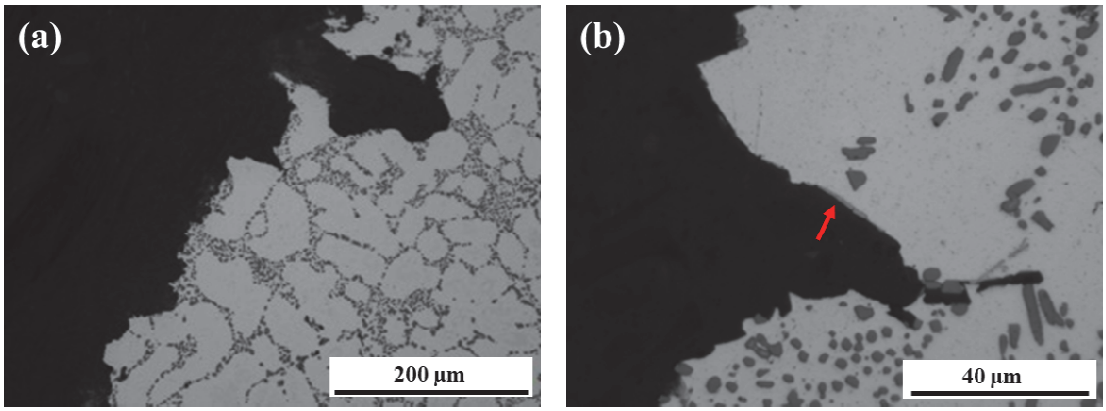

Figure 16: Fracture profiles of an impact strength A356-T6 specimen: (a) low magnification, (b) high magnification.

To support this assumption, in Fig. 16 are depicted two micrographs at different magnifications of the fracture profile of an A356-T6 impact strength specimen. Intermetallic compounds are scarcely found on the fracture profiles, even if some β-Al_5FeSi are present as pointed out in Fig. 16b (red arrow). The presence of these fractured platelet-like intermetallics is also confirmed by SEM/EDS analysis as shown in Fig. 17.

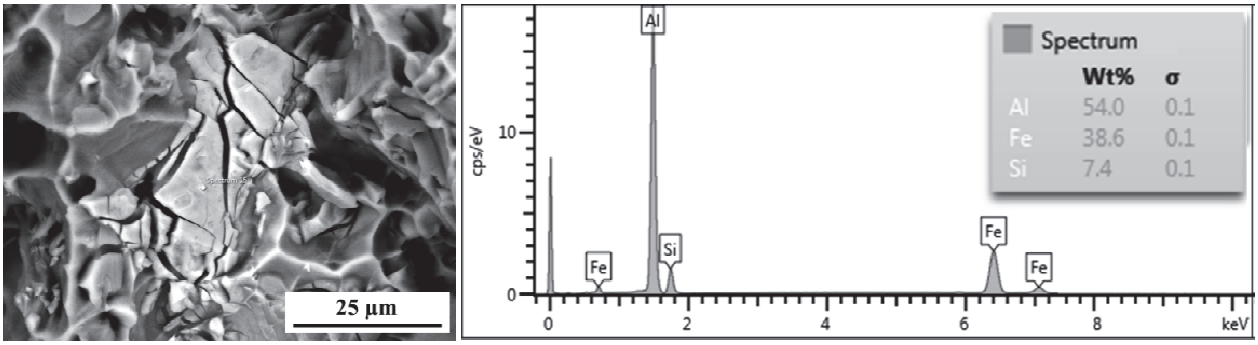

Figure 17: SEM micrographs of an impact strength A356-T6 specimen: fractured platelet-like intermetallic particle.

Nevertheless, a Si-driven intercrystalline fracture can be considered the main cause for fracture initialization; once a critical number of fractured particles is reached, the principal crack is formed by local linkage of close microcracks. Then, they propagate following a preferential interdendritic path, with a predominantly transgranular fracture mode and sometimes assisted by microporosities (Fig. 16 and Fig. 18).

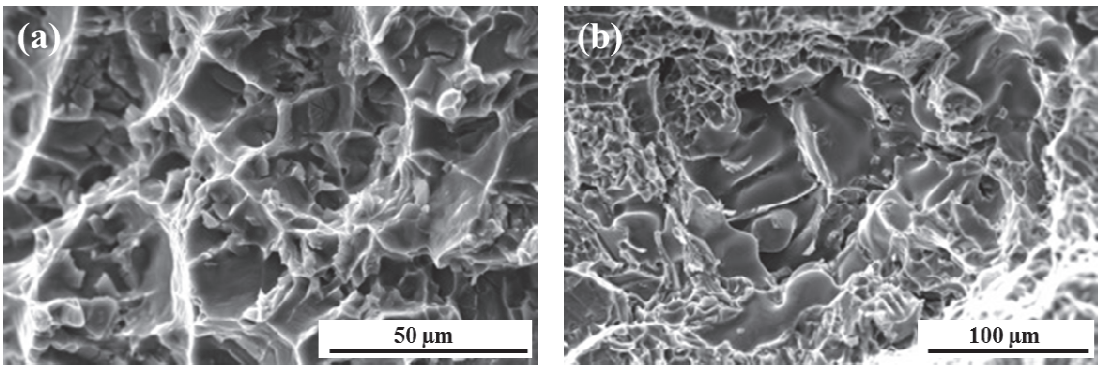

Figure 18: SEM micrographs of the fracture surface of an impact strength A356-T6 specimen: evidence of (a) dimples and fractured Si particles at high magnification and (b) microporosity.

Conclusions

The mechanical performances of AlSi3Cr alloy were evaluated in different heat-treated conditions in terms of tensile strength and impact toughness. Particular attention was paid to the influence of intermetallic phases on the mechanical performance of the material. In fact, the studied alloy is characterized by the presence of quite coarse intermetallic compounds that form due to the presence of Fe, Cr and Mn. The fracture mechanism was mainly ductile and intermetallic particles appear to play a marginal role in fracture initiation. Furthermore, the alloy shows remarkable tensile strength in most heat-treated conditions, while elongation can reach values very similar to that of the conventional A356 alloy for selected aged conditions. On the other hand, poor impact toughness values were measured because, in this case, intermetallic secondary phases act as crack initiation and propagation particles. This was demonstrated by the presence of coarse cracked intermetallic particles on the fracture surfaces in as cast and heat-treated conditions. Commercial A356 alloy exhibited impact toughness higher than AlSi3Cr alloy and the observations of fracture surfaces revealed a Si-driven main crack path, while intermetallic compounds were scarcely found.
Data collected in the present work provide interesting evidences of the important role played by intermetallic particles in the mechanical behavior of AlSi3Cr alloy, together with heat treatment parameters. The comparison with the commercial A356 casting alloy can be very helpful for the identification of proper applications for the studied innovative alloy.

Acknowledgments

This work has been supported by the Cariplo-Regione Lombardia funding [grant number E43J13001750007]. The authors would like to thank Maxion Wheels (Italy) for supplying the wheels. The authors gratefully acknowledge Mr. A. Coffetti for assistance in sample preparation and testing.

References

[1] http://www.european-aluminium.eu/media/1326/aluminium-in-cars-unlocking-the-lightweighting-potential.pdf, European Aluminium Association, Aluminium in Cars – Unlocking the light-weighting potential (2013).
[2] Zapp, P., Rombach, G., Kuckshinrichs, W., The future of automotive aluminium., Light Metals: Proc. TMS Annual Meeting, Warrendale, Pennsylvania, (2002) 1003-1010.
[3] Miller, W.S., Zhuang, L., Bottema, J., Wittebrood, A.J., De Smet, P., Haszler, A., Vieregge, A., Recent development in aluminium alloys for the automotive industry., Mater. Sci. Eng. A, 280 (2000) 37–49.
[4] Mahta, M., Emamy, M., Daman, A., Keyvani, A., Campbell, J., Precipitation of Fe rich intermetallics in Cr- and Co-modified A413 alloy, Int. J. Cast Met. Res., 18 (2005) 73-79.
[5] Shabestari, S.G., The effect of iron and manganese on the formation of intermetallic compounds in aluminum–silicon alloys, Mater. Sci. Eng. A, 383 (2004) 289–298.
[6] Taylor, J.A., Iron-containing intermetallic phases in Al-Si based casting alloys, Proc. Mat. Sci., 1 (2012) 19-33.
[7] Seifeddine, S., Johansson, S., Svensson, I.L., The influence of cooling rate and manganese content on the β-Al5FeSi phase formation and mechanical properties of Al–Si-based alloys, Mater. Sci. Eng. A, 490 (2008) 385-390.
[8] Kim, H.Y., Han, S.W., Lee, H.M., The influence of Mn and Cr on the tensile properties of A356–0.20Fe alloy, Mater. Lett., 60 (2006) 1880–1883.
[9] Sjolander, E., Seifeddine, S., The heat treatment of Al–Si–Cu–Mg casting alloys, J. Mater. Process. Tech., 210 (2010) 1249-1259.
[10] Wang, Q.G., Davidson, C. J., Solidification and precipitation behaviour of Al-Si-Mg casting alloys, J. Mat. Sci., 36 (2001) 739-750.
[11] Li, R.X., Li, R.D., Zhao, Y.H., He, L.Z., Li, C.X., Guan, H.R., Hu, Z.Q., Age-hardening behavior of cast Al–Si base alloy, Mater. Lett., 58 (2004) 2096-2101.
[12] Tocci, M., Donnini, R., Angella, G., Pola, A., Effect of Cr and Mn addition and heat treatment on AlSi3Mg casting alloy, Mater. Charact., 123 (2017) 75-82.
[13] Tocci, M., Pola, A., La Vecchia, G.M., Modigell, M., Characterization of a New Aluminium Alloy for the Production of Wheels by Hybrid Aluminium Forging, Procedia Engineer., 109 (2015) 303-311.

[14] Davis, J.R., ASM Speciality Handbook, Aluminum and Aluminum Alloys, ASM International, Materials Park, OH, (1993).
[15] Drouzy, M., Jacob, S., Richard, M., Interpretation of tensile results by means of Quality Index and probable yield strenth, Int. Cast Met. J., 5 (1980) 43-50.
[16] Mondolfo, L.F., Aluminum Alloys. Structure and Properties, Butterworth & Co Publishers Ltd, (1976).
[17] Li, Y., Yang, Y., Wu, Y., Liu, X., Supportive strengthening role of Cr-rich phase on Al–Si multicomponent piston alloy at elevated temperature, Mater. Sci. Eng. A, 528 (2011) 4427–4430.
[18] Timelli, G., Lohne, O., Arnberg, L., Laukli, H. I., Effect of Solution Heat Treatments on the Microstructure and Mechanical Properties of a Die-Cast AlSi7MgMn Alloy, Metall. Mater. Trans. A, 39A (2008) 1747-1758.
[19] Jorstad, J.L., Understanding sludge, Die Casting Engineer, (1986) 30-36.
[20] Gobrecht, J., Ségrégations par gravité du fer, du manganèse et du chrome dans les alliages aluminium-silicium de fonderie, Fonderie, 367 (1977) 171-173.
[21] Ferraro, S., Fabrizi, A., Timelli, G., Evolution of sludge particles in secondary die-cast aluminium alloys as function of Fe, Mn and Cr, Mater. Chem. Phys., 153 (2015) 168-179.
[22] Tocci, M., Pola, A., Montesano, M., Merlin, M., Garagnani, G.L., La Vecchia, G.M., Tensile behavior and impact toughness of an AlSi3MgCr alloy, Proc. Struct. Int., 3 (2017) 517–525.
[23] Zhang, D.L., Zheng, L.H., StJohn, D.H., Effect of a short solution treatment time on microstructure and mechanical properties of modified Al–7 wt.% Si–0.3 wt.% Mg alloy, J. Light Met., 2 (2002) 27–36.
[24] Warmuzek, M., Aluminum-Silicon Casting Alloys - Atlas of Microfractographs, ASM International, Materials Park, Ohio (2004).
[25] Park, D.S., Kong, B.O., Nam, S.W., Effect of Mn-dispersoid on the low-cycle fatigue life of Al-Zn-Mg alloys, Metall. Mater. Trans. A, 25A (1994) 1547-1550.
[26] Dowling, J.M. ,Martin, J.W., The influence of Mn additions on the deformation behaviour of an Al-Mg-Si alloy, Acta Metall., 24-12 (1976) 1147-1153.
[27] Elsebaie, O., Samuel, A.M., Samuel, F.H., Effects of Sr-modification, iron-based intermetallics and aging treatment on the impact toughness of 356 Al–Si–Mg alloy, J. Mater. Sci., 46 (2011) 3027-3045.
[28] Dieter, G.E., Mechanical metallurgy, McGraw Hill, UK, (1986).
[29] Smallman, R.E., Ngan, A.H.W, Physical metallurgy and advanced materials, Butterworth Heinemann, Boston, (2007).
[30] Merlin, M., Timelli, G., Bonollo, F., Garagnani, G.L., Impact behaviour of A356 alloy for low-pressure die casting automotive wheels, J. Mater. Process. Tech., 209 (2009) 1060-1073.
[31] Elsebaie, O., Samuel, A.M., Samuel, F.H., Effects of Sr-modification, iron-based intermetallics and aging treatment on the impact toughness of 356 Al–Si–Mg alloy, J. Mater. Sci., 46 (2011) 3027-3045.